I&EC research
Industrial & Engineering Chemistry Research

Open Access
This article is licensed under CC-BY 4.0

pubs.acs.org/IECR
Article

Butene Isomerization on Palladium Surfaces: Time-Dependent Monte Carlo Studies

Published as part of Industrial & Engineering Chemistry Research virtual special issue "Dmitry Murzin Festschrift".

Francesco Ferrante, Marco Bertini, Laura Gueci, and Dario Duca*

Cite This: *Ind. Eng. Chem. Res.* 2023, 62, 20608−20621

Read Online

ACCESS | Metrics & More | Article Recommendations | Supporting Information

ABSTRACT: A new time-dependent Monte Carlo approach, tdMC, is presented. This allows one to manage the quantum-chemical information relating to surface catalytic processes and rationalize, with atomistic dynamical perspectives, the corresponding reaction mechanism by providing descriptors that can be compared with experimentally obtained data. The approach, which falls into the more general microkinetic paradigm, is strictly self-consistent as it exploits information framed in just one computational method based on the density functional theory. The results simulated by the tdMC algorithm concern the isomerization of but-1-ene to *cis*- and *trans*-but-2-ene on Pd surfaces. This reaction was chosen mainly to focus on the development and implementation of the model as well as to point out the characteristics of the code and the soundness of the approach. In order to reach these goals, the simulated findings were compared to related experimental and computational literature data. From the study, it clearly emerges that the tdMC approach, although conceptually very straightforward and simple, is flexible enough to pinpoint the main characteristics of the reaction, which is just seemingly elementary and conversely governed by a complex mechanism involving, besides isomerization, even hydrogenation and dehydrogenation processes. Noticeably, new insights into the title reaction were also provided by the proposed approach.

INTRODUCTION

Kinetic and time-dependent Monte Carlo, tdMC, algorithms, aimed at performing realistic simulations of dynamic systems and actually being able to mimic the time dependence of stochastically studied physical phenomena, were introduced in the literature in the early 1990s.[1,2] These kinetic applications, developed in the frame of the Monte Carlo, MC, paradigm, were generally apt to conjugate the microscopic and macroscopic perspectives of molecular dynamics and of the conventional MC regime, respectively.[3] In the same years, Monte Carlo algorithms able to dynamically mimic catalytic reactions on metal surfaces were developed independently.[4] The latter were only subsequently explicitly defined as tdMC[5] simulation codes, but implicitly they had already employed, at the early implementations, the same basic concepts as the tdMC codes used in other scientific and technical contexts.[6]

In catalysis, tdMC codes have been used in the study of the hydrogenation of olefins[4] and their derivatives[7] when occurring on metal surfaces, as well as to investigate, within the class of the reactions above, occurrences that were generally not plainly taken into consideration but which are generally arising on the catalyst surface along with the main transformations. Important examples are (i) parallel hydrogenation of different fragments and substrates—clearly related to regio- and chemo-selectivity phenomena—(ii) isomerization, (iii) polymerization, and (iv) the formation of carbonaceous deposits.[8] In studying these processes, it became evident that there was a need to have a sound and common basis concerning the information on the reactants, surface species, transient intermediates, transition states, and products involved in the reactions. This common basis information clearly determines a way for constructing a set of event probabilities that are mutually consistent and capable of managing occurrences routinely less considered, such as diffusion and steric hindrance of the surface species or their potential effects on the surface events.[9] Therefore, the use of surface event energies and process descriptors of unrelated origin[4] has been progressively replaced by the use of information coming mainly from one common source, namely from quantum-chemical computations.[7−10]

By using the tdMC approaches, with the simulations of the catalytic processes, it has been possible to calculate experimental descriptors such as the turnover frequency, the selectivity to the formation of given species, their reaction order, as well as the apparent activation energy of a whole process. Furthermore, more exotic parameters could be extracted by tdMC simulations.

Received: July 21, 2023
Revised: September 20, 2023
Accepted: October 23, 2023
Published: November 20, 2023

Downloaded via UNIV DEGLI STUDI DI PALERMO on December 7, 2023 at 07:12:07 (UTC).
See https://pubs.acs.org/sharingguidelines for options on how to legitimately share published articles.

ACS Publications
© 2023 The Authors. Published by American Chemical Society

https://doi.org/10.1021/acs.iecr.3c02512
Ind. Eng. Chem. Res. 2023, 62, 20608−20621

Among these are, for instance, the ones associated with (i) the sticking probability of molecules hitting a surface from the gas phase, (ii) the steric hindrance of the reacting surface species, (iii) the structure sensitivity of a reaction, and (iv) the unexpected positive effects of the aging of given metal catalysts on their selectivity. In the tdMC applications, the fitting parameters, functional for adjusting the simulated trends to the experimental ones, have been significantly reduced over time.[9] Despite this, important properties, as already stressed, have been identified, and phenomena hardly interpretable, such as adsorption-assisted desorption[11] or the mechanism of the formation of hot atoms[12] on the surface of given metals, have been explained.[9]

The use of other dynamic or kinetic Monte Carlo, kMC, codes[13] is clearly related to that of the tdMC ones.[9] Although kMC was introduced later in the catalytic literature,[14] its development was nevertheless more continuous in the time as was its use.[15] The latter significantly may be associated with studies of catalyst design and active site optimization[16] and, more specifically, studies of industrial catalytic reactions such as methane reforming and CO oxidation processes.[17]

Hydrocarbon transformations on metal surfaces are usually considered simple reactions, and for this reason, they have also been considered introductory processes in the modeling and illustration of surface mechanisms at a didactic level.[18] On the other hand, these reactions and, in particular, isomerizations are remarkable from either the academic[19,20] or industrial[21,22] perspective and represent important branches in the more complex hydro-isomerization processes too.[23] The stoichiometric simplicity of the olefin isomerization processes and the significance of the coupled catalytic applications oriented us to the choice of the latter to picture the present tdMC algorithm/code, hereinafter designated as BACK.

In the next section, computational details—the quantum-chemical methods and codes used to obtain the basic information employed in the tdMC simulations—are illustrated with the tdMC algorithm and the physicochemical models mimicked. The results of the simulations are discussed in the following section—Results and Discussion—and, there, they are compared with both experimental and computational literature findings. New insights and perspectives on but-1-ene isomerization are finally furnished in the same section.

COMPUTATIONAL DETAILS

Quantum-Chemical Methods and Codes. The system used as a model for the catalyst is a three-layer 5 × 5 slab of palladium atoms cut from the fcc structure of the bulk and showing either the {111} or {100} surface. In the first case, the slab is characterized by supercell vectors with lengths equal to 11.192 Å in the x and y directions and angles of 90, 90, and 120°; for the {100} slab, the lengths above are 11.871 Å, while all the angles are equal to 90°. Normal to the slab, a vacuum of 30 Å was placed in each case. The size of the supercells allows for the avoidance of spurious interactions between the adsorbed/reacting molecule and its periodic image.

All geometry optimizations, relating to minima and transition states, were performed by using density functional theory, DFT, with the Perdew−Burke−Ernzerhof, PBE, exchange−correlation functional, in the spirit of the SIESTA approach.[24] New generation pseudopotentials, taken from the database of the PseudoDojo project[25] and including relativistic scalar effects, were employed and used in PSML format; the valence double-ζ quality plus polarization numerical basis sets joined to the pseudopotentials were generated with an energy shift equal to 0.005 Ry. The use of the PSML format for the pseudopotentials required PSML support for the SIESTA code, included in the SIESTA-PSML-R1 version.[26]

The Empathes code[27,28] was employed for the identification of the Transition States, TS. Empathes implements the Climbing Image Nudged Elastic Band, NEB, method[29,30] and provides an interface to the SIESTA program. For the NEB calculations, six images, generated using the image-dependent pair potential approach and connected to each other by dynamic springs, were considered sufficient. A threshold of 0.003 hartree/Å on the norm of atomic forces was set for the convergence of the NEB.

Physico-Chemical Models and Time-Dependent Code. The but-1-ene isomerization on palladium in the absence of hydrogen has been taken as a reaction example. The dynamic evolution of the events involved in the simulated isomerization processes was constantly evaluated by the BACK, **Blast Activated Chemical Key**, code based on the homonym tdMC algorithm. Specifically referring to the heterogeneous catalysis of gas/solid systems, the basic idea that characterizes the development of the model is particularly simple: a local **blast** of energy, originating from a collision of a molecule coming from the gas phase, has to occur in order to **activate** a **chemical key** event on a catalytic surface. This hypothesis already used to study surface phenomena,[9] even if not explicitly remarked, can be thought of as the basis of a successful series of Monte Carlo models applied to catalytic systems, referable to the pioneering work of Ziff et al.[31,32]

Supposing observation of a catalytic surface, this will indeed be characterized by empty sites and/or sites occupied by species that can transform and that can incidentally return to the gas phase. Both of these sets of surface-sites—singly constituted by sites or groups of sites, which in the following will also be called catalytically active surface units[33]—can be hit by a reactant, one of the possible products, or even a molecule of the eluant gas used to dilute, i.e., to regulate the partial pressure of the reactant. A simplification introduced for speeding the simulations—that, however, is not mandatory and factually irrelevant in the interpretation of the results—is represented by the impossibility that the molecules produced during the process hit, hence readsorb, once they left the surface. This simplification originates from the very low concentration of these species in the gas flow due to the hypothesized occurrence of the processes under the continuously renewed gas phase.

When a reactant molecule hits empty sites on the surface, it may or may not adsorb. This depends on the activation barrier value, if present, and the energy characterizing the impinging molecule. The fraction of molecules of kind α that can be adsorbed is therefore determined by an adsorption probability, Π^{α}_{ads}. This is calculated by integrating the tail of a Boltzmann energy distribution

$$2\left(\frac{1}{k_B T}\right)^{3/2} \int_{\varepsilon_\alpha}^{\infty} \sqrt{\frac{E}{\pi}} \exp\left(-\frac{E}{k_B T}\right) dE$$

where ε_α represents the minimum energy possessed by molecule α to overcome a possible energy barrier required for its adsorption, T is the considered temperature, and k_B is the Boltzmann constant—and normalizing the result, dividing by the value of the same integral for $\varepsilon_\alpha = 0$

https://doi.org/10.1021/acs.iecr.3c02512
Ind. Eng. Chem. Res. 2023, 62, 20608−20621

$$\Pi_{ads}^{\alpha} = \frac{\int_{\varepsilon_\alpha}^{\infty} E^{1/2}\exp\left(-\frac{E}{k_B T}\right)dE}{\int_{0}^{\infty} E^{1/2}\exp\left(-\frac{E}{k_B T}\right)dE} \quad (1)$$

The frequency of hitting characterizing any reference α species per catalytically active surface unit is

$$f_h^{\alpha} = f_\xi \frac{p_\alpha}{\sqrt{2\pi m_\alpha k_B T}} \quad (2)$$

where m_α is the molecular mass of the gas α hitting the surface, p_α is its partial pressure, and f_ξ is the conversion factor that depends on the extension of the surface unit above, which reduces the dimensions of f_h from $[m^{-2}\ s^{-1}]$ to $[s^{-1}]$. With N the number of catalytically active units of a surface, Nf_h^{α} is used by BACK for stating the time elapsing, see ref 4a, computing the colliding α molecules from the gas phase on the surface.[1] The sticking probability of the molecule α, σ_α, is monitored by BACK, counting the number of adsorbed molecules on the surface, ν_{ads}^{α}, with respect to their collision number, $\nu_{hit}^{\alpha} = Nf_h^{\alpha}\Delta t$, in a given time interval Δt [s]. Hypothesizing just monolayer formation, ν_{ads}^{α} depends on the unoccupied surface unit fraction, θ_0, and adsorption energy barrier of α: $\nu_{ads}^{\alpha} = \nu_{hit}^{\alpha}\Pi_{ads}^{\alpha}\theta_0$; hence, $\sigma_\alpha = \nu_{ads}^{\alpha}/\nu_{hit}^{\alpha}$ proves to be a function of time due to its dependence on θ_0.[9,34] When the surface begins to populate with the reagent species, they transform, originating the different derivatives of the reaction *panorama*, i.e., all the species characterizing the process. In any case, the following relationship will be valid: $\sum_{i=0}^{n}\theta_i = 1$; with θ_i, for $i \neq 0$, the fraction of the catalytically active surface unit occupied by the i-th species and n the number of different surface species.

All the i-th species, including the 0-th one, are considered as pseudoisomers.[35] These are characterized by both a fixed number of metal surface atoms, corresponding to the atoms of the catalytically active surface units, and a set of atoms referable either to the adsorbed substrates or to the gas phase species. These pseudoisomers mutually transform during the reaction, and the corresponding θ_i values are monitored and self-updated by BACK.[2]

It is here recalled that one of the main peculiarities of the present tdMC model is represented by the point concerning the pseudoisomers above. Another significant point concerns the absence of a matrix explicitly mimicking the catalytic surface.[4,31,36] Both of these features speed up the selection and reorganization processes of the surface species involved.

From the starting assumptions on BACK, for a given pseudoisomer l to be converted into the k one, being l and k separated by a given energy barrier, it is necessary that the species l is hit by a molecule coming from the gas phase, which owns sufficiently high energy to overcome the involved activation energy, hence to activate the transformation process $l \rightarrow k$. It is clear that this event may compete with others; in this case, a random number generator (RNG) determines the outcome of the occurring event. RNGs[37] are fundamental in any MC simulation, being employed whenever a choice between several options is required. For details see Scheme S1, reported as Supporting Information, where the RNG use is highlighted in the flow chart of the code.

The relative probability, Π, that a given species k, originating from l, is transformed in j, which is one among any of the obtainable different species i by a forward process, is calculated by[3]

$$\Pi_{k\rightarrow j} = \frac{\exp\left(-\frac{\varepsilon_{kj}-\varepsilon_{kl}}{k_B T}\right)}{1+\sum_{i\neq l}\exp\left(-\frac{\varepsilon_{ki}-\varepsilon_{kl}}{k_B T}\right)} \quad (3)$$

where, as illustrated by the following Scheme 1, ε_{ki}, ε_{kj}, and ε_{kl} are the energy barriers characterizing processes, in which k is invariably the starting species.

Scheme 1. Fragment of a Generic Reaction Path. Species *l* is Transformed into the *k* One; the Latter Can Evolve into Different Species *i*, One of which is *j*. The Energy Barriers of the Different Reaction Events are Pointed Out by the *ε* Terms, Whose Subscripts Directly Individuate the Reaction Directions

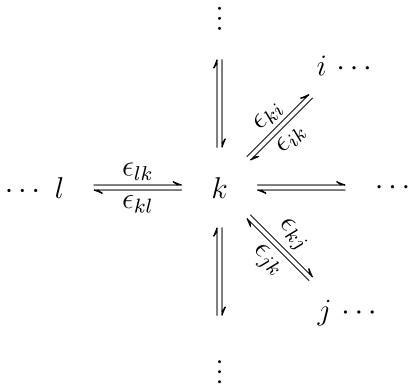

The first, ε_{ki}, is that of a generic i-th forward reaction bringing to any of the species i in which k can be transformed, while the second and third—ε_{kj} and ε_{kl}, respectively—those leading specifically to the given j-th species, following a forward reaction, and to the starting l-th species, by the only possible backward reaction. In the particular case, relating to the backward reaction $k \rightarrow l$, i.e., $j = l$, the relative probability becomes

$$\Pi_{k\rightarrow l} = \frac{1}{1+\sum_{i\neq l}\exp\left(-\frac{\varepsilon_{ki}-\varepsilon_{kl}}{k_B T}\right)} \quad (4)$$

Considering both eqs 3 and 4, it is possible to formalize the basis epistemic relationship $\sum_j \Pi_{k\rightarrow j} = 1$, valid for any k-th species and including among the j terms also the source species l. In order to contextualize, these probabilities are those managed by RNG4, see Scheme S1, to rearrange a selected pseudoisomer involved in the catalytic transformation.

During the simulations of the catalytic processes, the surface can undergo local changes that require the consideration of fresh pseudoisomers having different characteristics with respect to the starting one. The surface could, in fact, age or modify due to the production of species formed in the reaction; an example pertinent to the title, isomerization, is given by the formation of surface hydrogen in dehydrogenation processes, locally producing hyper-hydrogenated units. These changes are taken into account by defining new scenarios characterized by different pseudoisomers which evolve each other in parallel. In this case, the methodology previously described for modeling a single scenario is applied in parallel to multiple scenarios, with their occurrence determined by probabilities proportional to the relative surface-site quantities, each of which characterizes the respective scenarios. The choice of the scenario is managed by RNG0, see Scheme S1.

https://doi.org/10.1021/acs.iecr.3c02512
Ind. Eng. Chem. Res. 2023, 62, 20608−20621

Scheme 2. Reaction Paths of the Butene Isomerization: First, Up, and Second, Down, *scenario*. These are Distinguished for the Characteristics of the Catalytically Active Surface Units, Referable to the Starting (∗) and Hyper-hydrogenated (•) Sites, Respectively

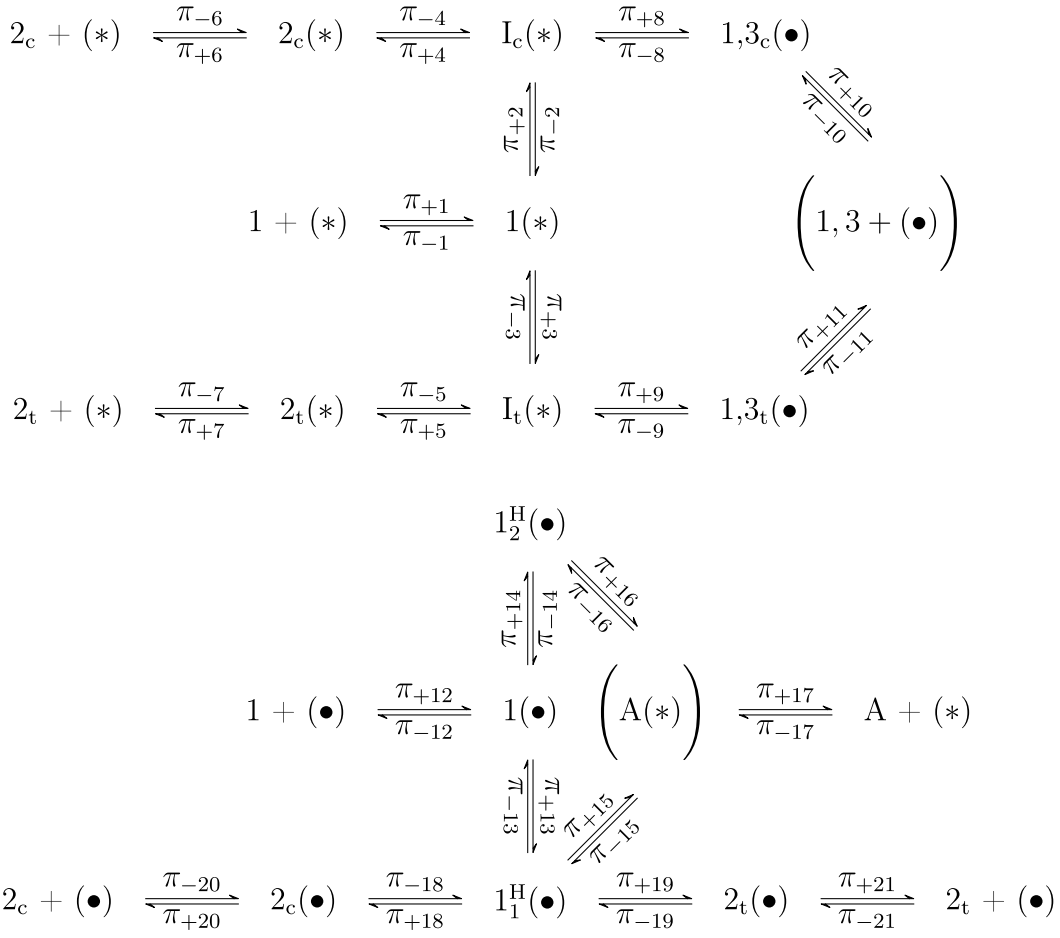

It is here to be stressed that all the ε values in eqs 3 and 4 are assumed to be known, and in the present work, they actually are the zero-point energy, ZPE, values obtained by quantum-chemical calculations in the frame of DFT, as summarized in the preceding subsection. In future studies, particularly those focusing on the microkinetic modeling of experimental catalytic outcomes, the free energies associated with the corresponding surface processes should be taken into consideration. This step aims to mitigate potential inaccuracies that could arise, possibly due to the neglect of entropic effects.[38]

Assuming that the surface transformations of the intermediate species imply negligible entropy variations,[39] in this work, the entropic effects will be accounted for by introducing just a single constant parameter, S_p, which facilitates the desorption of both reactants and products from the catalyst surface. A parameter acting oppositely might even be considered for adsorbing species in the case, which is not the present one, of activated surface uptake.

BACK takes into account each reactant molecule converted into a product and, normalizing the corresponding cumulative number to the number of sites actually present during the occurrence of the process and to the time elapsed, updates the turnover frequency, TOF $[s^{-1}]$.[4] If more than one species is produced, BACK also calculates the selectivity, S_α, with respect to one of them, e.g., α, from the ratio between the number of molecules α and the total number of molecules of all the species desorbed.[8]

An interesting aspect that is generally included in the treatment of surface processes concerns the effects of lateral interactions[1] and therefore of the steric hindrance of the different adsorbed species, see, for example, refs 4a and 9. These effects have been taken into consideration by introducing a hindrance parameter, h_p, that modifies the value of the minimum energy barrier for any event to take place. The h_p parameter, which, as the S_p one, reduces by a certain percentage the value of the activation barriers of the surface transformations, is introduced in the hypothesis that a surrounding steric pressure, produced by the molecular hindrance, is acting by the effect of the neighboring surface molecules on the species that is undergoing the transformation. The transforming species will therefore be characterized by a larger content of energy,[4,8,9] and they will need a smaller amount of energy to overcome the energy barrier of the considered transformation. In passing, it is worth noting that the "fitting" parameters h_p and S_p are the only ones not calculated quantum-chemically in the present tdMC model. Besides, the effects of both of these parameters are clearly consistent with each other, and they will therefore synergistically increase the probability of desorption of both reactants and products.

https://doi.org/10.1021/acs.iecr.3c02512
Ind. Eng. Chem. Res. 2023, 62, 20608−20621

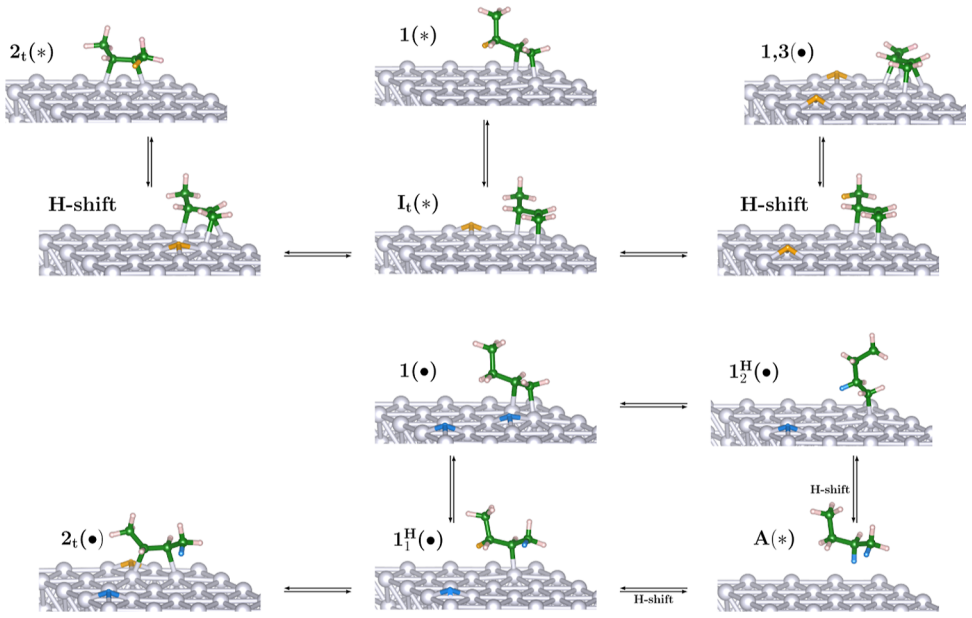

Figure 1. Optimized fragment of a selection of significant species (pseudoisomers) present on the Pd{111} surface: first (up) and second (down) scenarios. Species that interconvert each other freely are, as an example, those characterized by H shifts (in yellow) on the left and on the right with respect to $I_t(*)$. Hyper-hydrogenated fragments are characterized by surface hydrogen in blue.

Phenomena related to the diffusion of olefinic surface species have not been taken into consideration because their mixing effects are not significant on metallic surfaces.[4]

Scheme 2 pictures the reaction mechanism that, in agreement with the literature,[40,41] turned up by the DFT calculations and that will be used in the tdMC simulations. In the scheme, the catalytically active surface units defining the different scenarios are represented by (∗) and (•). Both of these are characterized by a consistent number of palladium atoms, with the former associated with pristine surface units and the latter linked to hyper-hydrogenated surface units. The hyper-hydrogenated units are generated through the dehydrogenation of butene molecules, leading to the formation of either *cis*- or *trans*-1,3-butadiene on the surface. Due to the easy H surface diffusion on Pd, the scenarios should be clearly interconnected. As a consequence, the background scenario in the system evolution at a given time of the simulation is chosen based on the fractions of pristine and hyper-hydrogenated surface units.

In the first scenario, 1, 2_t, and 2_c are 1,3 but-1-ene, *trans*- and *cis*-but-2-ene, and 1,3-butadiene, respectively. The adsorbed but-1-ene is species $1(*)$, while the two different surface intermediates that evolve into the *cis*- and *trans*-adsorbed species, $2_c(*)$ and $2_t(*)$, are the species $I_c(*)$ and $I_t(*)$, respectively. Both of them are allylic surface fragments of the general formula C_4H_7, with the corresponding pseudoisomers formed by the aforementioned C_4H_7 fragments and one H atom on the catalytically active surface units. The C_4H_7 surface fragments, as already mentioned, can even evolve into the adsorbed 1,3-butadiene, i.e., $1,3_c(•)$, *cis*- and $1,3_t(•)$, *trans*-species. In these cases, the residual catalytically active surface units, in which two hydrogen atoms remain, are the hyper-hydrogenated ones (•), characterizing the second scenario. Besides A, which corresponds to butane, formed by butene hydrogenation on hyper-hydrogenated surface units, the nonadsorbed species of the second scenario are the same as those of the first one. Clearly, the desorption of A restores the starting catalytically active surface units (∗). The different butenes when adsorbed on the hyper-hydrogenated site portions are represented by $1(•)$, $2_c(•)$, and $2_t(•)$. Finally, the surface intermediates $1_1^H(•)$ and $1_2^H(•)$ stand for adsorbed C_4H_9 monohydrogenated butene species in positions 1 and 2, respectively, see Figure 1.

Either $1(*)$ or $I_c(*)$ and $I_t(*)$ individually represent sets of different surface configurations having very close energy values. For this reason, they were solely considered surface species characterized by easy interconversions, occurring between the different arrangements almost without the involvement of energy. Interestingly, the interconversion between $I_c(*)$ and $I_t(*)$ proved to be very difficult, if not impossible, to take place. A selection of optimized surface fragments, referring to Scheme 2, are detailed in Figure 1.

The probability terms π_{+n} and π_{-n}, in Scheme 2, symbolize the probabilities of the occurrence of the corresponding forward and backward reactions in the pathway. Instead of probabilities, π, relative probabilities, Π, are nevertheless employed in the simulations. Relative probabilities Π, introduced by eqs 3 and 4, are obtained by appropriate ratios of the probabilities, π, which are assumed to be proportional to the values of k [s^{-1}], obtainable by the Eyring−Polanyi equation for the various events.[42] This procedure (i) decouples probabilities from time and (ii) avoids evaluating the transmission factors, κ terms, present in the Eyring−Polanyi equation, as they are assumed to be about constant for surface events originating from a common species and, as such, cancel out in evaluating the ratios. The null event probability, related to a set of inconsequential events, here represented by the Ar atoms hitting the surface, is also implicitly reckoned.[4]

Having focused on the catalytic process from the physicochemical point of view, it is now possible to frame it within the flow chart of BACK, detailed in Scheme S1. Code input, starting the flow chart and initializing the code run, consists of the morphostructural information on the catalyst and the energetic parameters regarding the surface species. In the input are also included the masses of the gas phase species,

https://doi.org/10.1021/acs.iecr.3c02512
Ind. Eng. Chem. Res. 2023, 62, 20608−20621

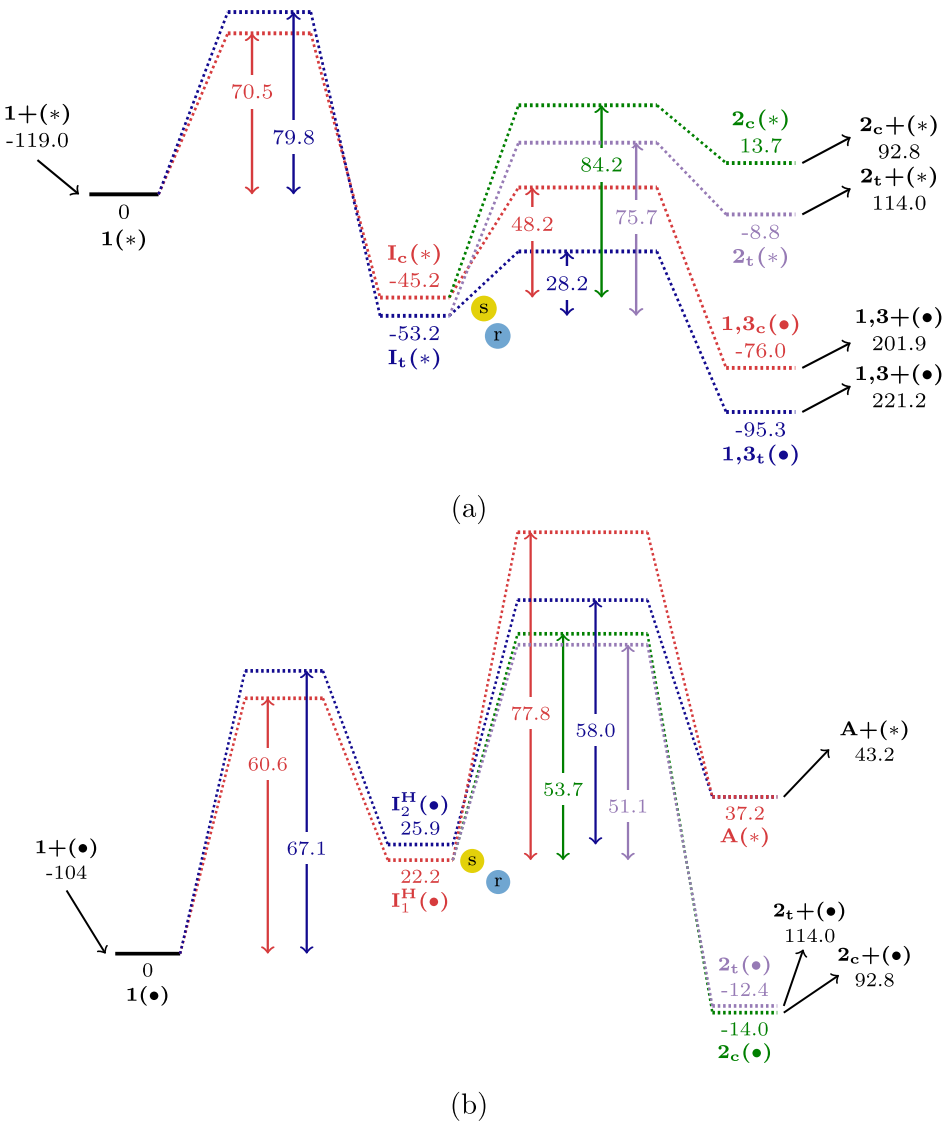

Figure 2. Energetics/kJ·mol^{-1} of the steps found on the Pd{111} surface in the first (a) and second (b) scenario; these match with the pathways of Scheme 2. Abstraction, AB, and addition, AD, mechanisms are related to the first and second scenarios, respectively. Symbols r and s inside the colored circles indicate the presence of molecular rearrangement and surface hydrogen shifting, related to surface fragments/pseudoisomers freely interconverting.

together with their partial pressure and the temperature considered in the simulation. These parameters determine, as already discussed, the hitting probabilities of the different gas phase species. In the initialization phase, the unit of time to be used during the simulation is calculated, while the characteristics of the surface and the degree of occupation of the surface units in relation to the different surface species are defined along with their probabilities of evolution in the other species individually connected to them. The fitting parameters, S_p and h_p, are finally defined while experimental descriptors—e.g., TOF, selectivities, and adsorbing species sticking probability—initialized and then updated with the surface properties during the simulation.

RESULTS AND DISCUSSION

Experimental Background. Simulations of experimental and computational data performed by tdMC applications from the literature on butene isomerization processes will be discussed in the following section. The results will make it possible to validate the inferences developed so far and to give a unifying perspective on the reaction mechanism at the atomistic level that is still missing. The following items summarize the most significant aspects of the processes under study:

(i) Irrespective of the presence of molecular H_2, the isomerization and hydro-isomerization processes on but-1-ene seem to begin with the addition of one surface hydrogen and end after the migration of the double bond by its subsequent release on the surface.[43]

(ii) Although different metal catalysts, either supported or not, usually show different relative reaction rates, their whole mechanisms are comparable, namely those relating to Pd and Pt-containing systems.[43]

(iii) The occurrence of two different surface mechanisms, AB and AD, could be hypothesized, depending on the respective starting reactions. The mechanism will be AB or AD if the reaction begins with an olefin H abstraction or addition, respectively. Surface fragments of π and/or π–allylic nature have a special role in the different mechanisms.[40]

https://doi.org/10.1021/acs.iecr.3c02512
Ind. Eng. Chem. Res. 2023, 62, 20608−20621

(iv) AB and AD mechanisms on metals are responsible not only for the isomerization processes but also for those referable to hydrogenation, e.g., with formation of butane,[41] and dehydrogenation, e.g., with the formation of 1,3-butadiene.[40,41] Furthermore, AB and AD pathways can occur in parallel, even changing their relative weight with the metal catalyst and being comparable only when Pd is specifically considered.[40]

(v) In the presence of just traces of hydrogen on Pd surfaces, the mechanism is preferentially AD.[44] There may be conditions for which stereoselectivity toward *cis*-but-2-ene isomer formation over the thermodynamically more stable *trans*-species is observed,[45] while the presence of hydrogen is mandatory to start the isomerization processes.[44]

Before proceeding further, it can be preliminarily observed that the mechanisms turning up from the DFT analysis are, on the whole, compatible with the experimental ones already introduced in the literature, whose main characteristics are outlined above. In particular, it can be pointed out that the AB and AD mechanisms can be identified with the first and second scenarios represented at the top and bottom in Scheme 2 and Figure 2.

tdMC Simulations. *Starting Evaluations.* Figure 2 shows the energetics of the different steps occurring in but-1-ene isomerization on the Pd{111} surface. The corresponding event probability values employed in the simulations at 463.15 K on Pd{111} surfaces are reported in Table S1 as Supporting Information.

Preliminarily, it is interesting to note that the present DFT calculations suggest that the AD mechanism, namely the one occurring on the hyper-hydrogenated surface units, represented at the bottom of Scheme 2 and Figure 2, cannot be initiated on {100} surfaces because of the inability of surface hydrogen to approach but-1-ene. This does not mean that the steps of the mechanism above cannot occur on Pd{100} surfaces; rather, it would indicate that these steps can take place following different mechanisms.

Actually, in the presence of a large excess of hydrogen, steps of the second *scenario*, i.e., of the AD mechanism, could occur, as an example, either by hydrogen adsorbed in the metal bulk, which then segregates near surface species able to capture hydrogen, or by diffusion at high temperatures of unsaturated species toward hyper-hydrogenated sites, always produced by bulk hydrogen segregation. These parallel mechanisms, for sure involving the presence of gas phase H_2, are not explicitly considered in this work, being its main focus the but-1-ene isomerization just in the absence of molecular H_2. On the other hand, the difference in the behavior of the palladium {100} and {111} planes implicitly allows one to infer that the title reaction has to be structure-sensitive, see ref 23d, favoring the {111} palladium plane activity in the but-1-ene isomerization when hydrogen is present on the surface. However, since it will be shown that the AD mechanism is requisite for the occurrence of but-1-ene isomerization in the absence of molecular H_2, the reaction on the {100} plane will not be further considered.

Scheme 3 shows an experimental design graph, *edg*, aimed at rationalizing the effects of h_p, S_p pairs on the but-1-ene isomerization on palladium {111} facets. The points individuate parameter pairs used in the simulations. The values of the h_p parameter are shown on the abscissa and those of S_p on the ordinate; thus, the lowest point in the graph, for instance, individuates simulated processes, collectively called 0500 models, characterized by the pair of values h_p = 0.5, S_p = 0.0. If not explicitly said, simulations were carried out at 4 different temperatures, 373.15, 403.15, 433.15, and 463.15K, keeping the partial pressure of but-1-ene constant at 0.05 atm and the total pressure, including Ar, equal to 1 atm. A model surface of 3500 sites, implicitly characterized by periodic boundary conditions, was considered. As an example, it is finally stated here that the simulation at 403.15 K, exerting the parameters of the central point in the experimental design of Scheme 3, is denoted as the 0505@403 model, with the other simulations, discussed in the following, indexed accordingly.

Scheme 3. Experimental Design Aimed at Isolating h_p, S_p Pairs Able to Mimic Reference Literature Data. Cyan and Purple Points Fix Significant and Not Significant Models, Respectively. Violet Points Individuate Simulated Systems Able to Reproduce Literature Data, but, on the Whole, Considered as Matching with Less Significant Models

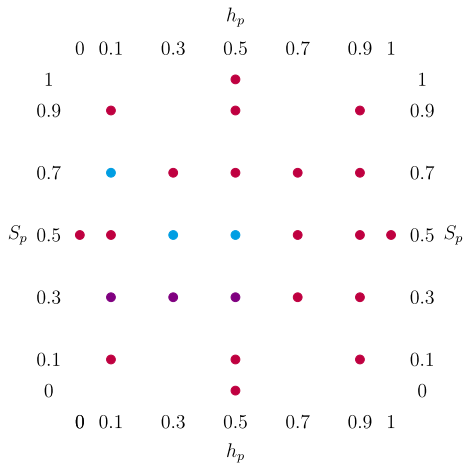

To assess the robustness of the approach, simulated findings corresponding to the *edg* were actually compared with the literature data. In detail, steady-state TOF values were determined at various temperatures using the BACK code, and the apparent activation energy parameters, Ea_{app}, were calculated by fitting the sets of TOF vs $1/T$ values for different h_p and S_p pairs using the Arrhenius equation.[46] The mimicked TOF and Ea_{app} parameters, reported with the corresponding literature data as Supporting Information in Table S2, have been thus used along with the simulated selectivity descriptors of Table 1, i.e., cis/trans stereoselectivity, $SS_{c/t}$,[43−45] and selectivity to butane and 1,3-butadiene, S_a and $S_{1,3}$, to guess the soundness of the h_p, S_p couples by comparing modeled and literature, activity and selectivity, parameters determined in consistent reactivity conditions.

In passing, it is here recalled that either hydrogenation or dehydrogenation of but-1-ene, related to the produced amount of butane and 1,3-butadiene, has been less investigated when the isomerization is conducted in the absence of molecular H_2 due to the trace size of the formed species. At variance with that, the stereoselectivity parameter is particularly sensitive (i) to the conditions of use of the catalyst and (ii) to the nature of the support eventually present.[43] In particular, $SS_{c/t}$ increases with decreasing the presence of hydrogen[44] and with increasing the partial pressure of but-1-ene, being the role of the temperature less detailed.[45] As an example, the particular working conditions used by Carrà and Ragaini[45] allowed them to identify

https://doi.org/10.1021/acs.iecr.3c02512
Ind. Eng. Chem. Res. 2023, 62, 20608−20621

Table 1. Simulated cis/trans Stereoselectivity, $SS_{c/t}$, and Selectivity to Butane and 1,3-Butadiene, S_a and $S_{1,3}$, Respectively, at 373.15 K Obtained by Models Having Different h_p, S_p Pairs

	models						
selectivities	0103	0107[a]	0303	0305	0503	0505	0703
$SS_{c/t}$	0.4(3)	7.(3)	0.4(3)	0.4(4)	0.4(2)	0.4(3)	0.4(2)
S_a	0.008	0.000	0.007	0.007	0.007	0.007	0.005
$S_{1,3}$	0.007	0.000	0.009	0.007	0.020	0.009	0.094

[a]Selectivities were determined at 433.15 K in order to be comparable to those reported in ref 45.

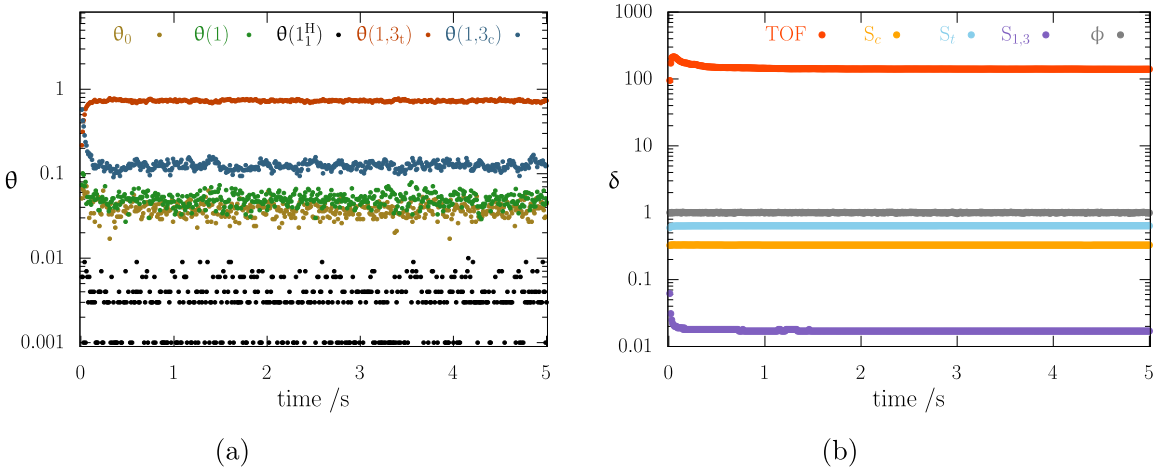

Figure 3. tdMC output of the 0305@463 model: (a) molar ratio of empty surface units, θ_0, and of significant surface derivatives summarized by the symbol θ, whose details are given using the inset symbols, and (b) activity and selectivity descriptors, δ vs time [s]. Symbol δ, beside TOF, and the fraction of hyper-hydrogenated catalytically active surface units, ϕ, summarize the selectivities to different species.

characteristic values of $SS_{c/t} > 1$ attributable to the presence of two different surface mechanisms, one of which prevailing on the other. Besides this literature datum, which in any case represents a *unicum*, it is generally agreed however that the *trans*-species prevails over the *cis*-one[21,44] with relative quantities that, to varying degrees, approximate the ratio 2:1, $SS_{c/t} \approx 0.5$.[43,47]

The simulated findings are related in a simple way to the coloring of the points in Scheme 3.[48] In fact, the models 0107, 0305, and 0505, represented as cyan points in the scheme, as well as the models 0103, 0303, and 0503, represented in violet, apparently identify meaningful systems. They are distinguished, however, for reasons that will be deepened in the next section. The remaining models, in purple in Scheme 3, are characterized by values of Ea_{app} and/or TOF at 373.15 K either not detectable at the simulated condition or pretty different with respect to the experimental references. In both cases, these models were related to nonsignificant physical conditions.

It is recalled that in grouping these models, in addition to the Ea_{app} and TOF parameters of Table S2, the values of $SS_{c/t}$ as well as those of S_a and $S_{1,3}$, at 373.15 K were also taken into account. With respect to this, S_a and $S_{1,3}$, smaller than 0.01 for the first parameter and in between 0.01 and 0.02 for the second were considered admissible.[40,41] In order to assign significance to a given modeled system, the different selectivities shown in Table 1 for selected systems clearly become discriminating when the Ea_{app} and TOF values are borderline. The analysis of the table explains in particular the exclusion of the 0703 model, showing acceptable activity parameters; see Table S2, but a very large $S_{1,3}$ value. Regarding the $SS_{c/t}$ parameter, it should be noticed that all the values reported in Table 1, but those corresponding to the model 0107@433, are always slightly larger than 0.4, very close to the experimental result, ca. 0.5 at 373.15 K. On the other hand, model 0107@433 is an interesting system showing an $SS_{c/t}$ value comparable to that reported by Carrà and Ragaini[45] at 433.15 K, which is ≈ 5.

Figure 3, obtained by applying the probabilities of Table S1, explains the basics of the following analysis based on the tdMC simulation findings. At first, it is useful to say that figures like this one show instantaneous values of descriptors related to surface events, occurring every one hundredth of a second. Furthermore, at the pressure and temperature generally considered in this work, the order of magnitude of the number of events simulated per surface unit between two points is $\approx 2 \times 10^5$, each occurring about every 0.05 μs of simulated time. In Figure 3, box 3a shows both the relative abundance of significant surface derivatives and the achievement of the steady-state conditions of the whole system through the evaluation of the surface molar ratio, θ, of the same derivatives.

The relative abundance, namely of but-1-ene, $\theta(1)$, cis and trans 1,3-butadiene, $\theta(1,3_c)$ and $\theta(1,3_t)$, and of the mono-hydrogenated butene, $1^H_1(\bullet)$, surface derivative, $\theta(1^H_1)$, is, for example, useful to correlate the surface population with the activity and selectivity outcomes presented in box 3b. In respect to this, it should be noticed that the θ values of butane and of the larger part of the remaining species have, if not explicitly underlined, values equal to zero or anyway less than 0.001; hence, for the sake of simplicity, they are not usually shown. In details, box 3b shows the selectivity values to cis and trans but-2-ene and to 1,3-butadiene S_c, S_t and $S_{1,3}$, along with the TOF relating to the disappearance of but-1-ene, and the fraction of hyper-hydrogenated surface units, ϕ. The latter is included among the activity descriptors because its value clearly directs the reactivity toward one or the other scenario.

https://doi.org/10.1021/acs.iecr.3c02512
Ind. Eng. Chem. Res. 2023, 62, 20608−20621

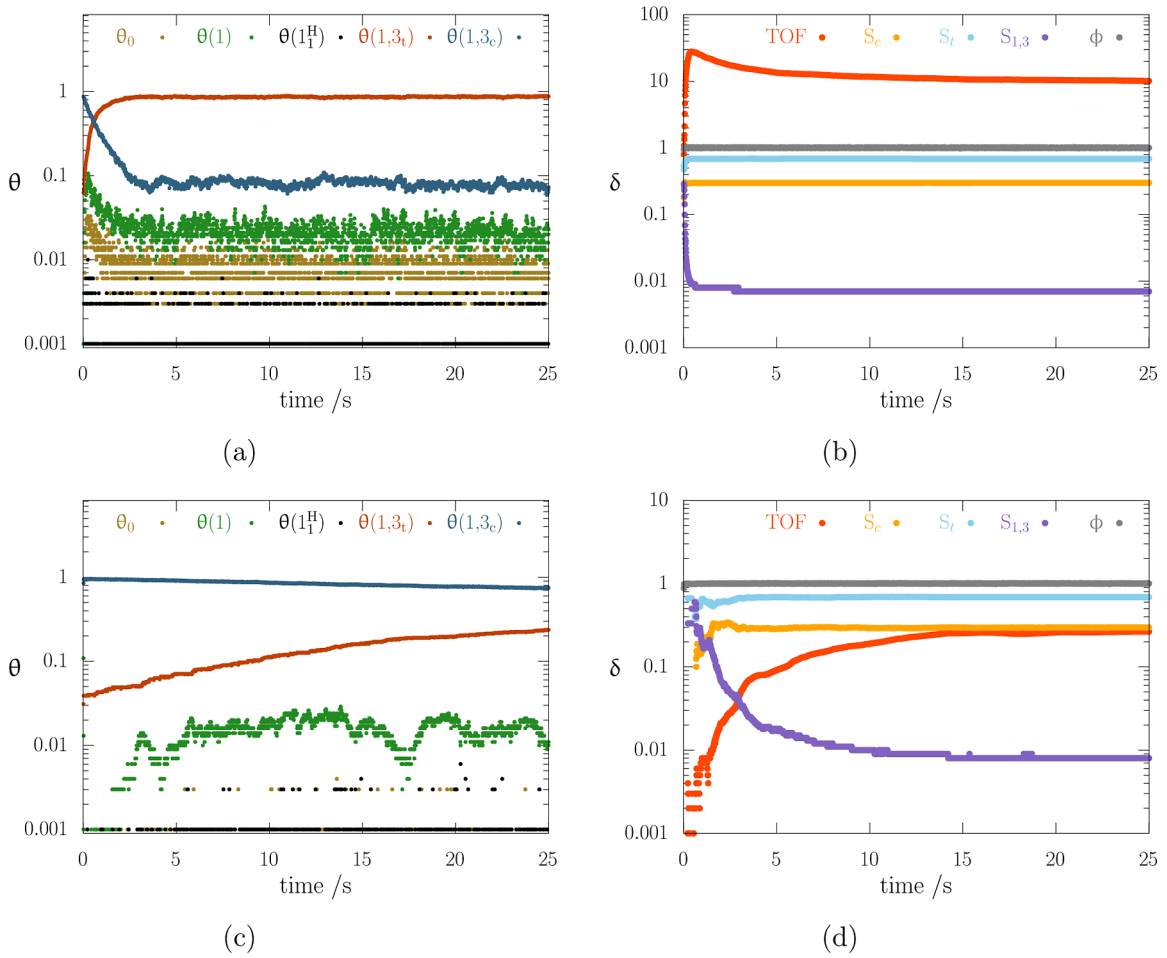

Figure 4. Descriptors θ and δ for the 0305@373—(a,b) at the top—and 0505@373—(c,d) at the bottom—models: inset symbols show the simulated descriptors, the behaviors of which are represented. Both of these models are characterized by $SS_{c/t} < 1$.

Analysis. From the analysis of Table S2 and Scheme 3, it emerges that only a limited number of h_p, S_p pairs allow for the identification of physically meaningful systems. However, on the whole, it can be remarked that the experimental data are well reproduced by some of these pairs.

It is interesting to mention that beyond the physical meaning that can be attributed to the h_p and S_p descriptors, they still determine analyzable surface conditions for a given system, which can be associated with the simulated results of catalytic activity and selectivity for the same system. Thus, it is possible to attempt a correlation between surface properties and macroscopic evidence in terms of activity and selectivity, regardless of the physical meaning of the employed descriptors. This can, for example, help understand why $SS_{c/t}$ changes, even inverts, in the isomerization of but-1-ene in the absence of H_2, as the surface population of a catalyst changes during the catalytic transformation. With this in mind, the following discussion focuses on the most significant models useful for assessing the analytical capabilities of the proposed approach.

Figure 4 shows the surface populations of species having θ values larger than 0.001, along with the corresponding activity and selectivity values for the species produced during the simulated isomerization when using the 0305@373 and 0505@373 models. Tables S2 and 1 show how these models are capable of reproducing the experimental descriptors TOF and Ea_{app}, as well as the various selectivities that can be taken as experimental references. Furthermore, it can be observed, in line with what is generally found, that the surface molar ratio of unoccupied surface units, θ_0, has negligible values when the process reaches the steady state. Irrespective of the considered model and the ways in which the adsorbed 1,3-butadiene species arrange on the surface, it can still be observed that the same surface is consistently covered by a certain quantity of but-1-ene and a smaller amount of its monohydrogenated derivative, $1^H_1(\bullet)$, which feeds the isomerization process. Of course, given the absence of other surface intermediates, the surface reaction, originating with a value of $SS_{c/t} < 1$, should mainly occur in the second scenario, i.e., through the AD mechanism.

An important feature of these systems is the presence of hyper-hydrogenated surface units that reach 100% relative presence in the early stages of the surface reaction. The result is noteworthy and in agreement with the literature data.[41,45] In fact, Carrà and Ragaini[45] had already hypothesized that $SS_{c/t} < 1$ could be linked to an excess of hydrogen in the reaction environment, while Ragaini[41] suggested that out of the two mechanisms, AB and AD, the AD one, i.e., the second scenario, could be activated by hydrogen originating from the dehydrogenation of but-1-ene, leading to the formation of 1,3-butadiene derivatives on the surface.

The systems 0103, 0303, and 0503 are shown to be able to reproduce both the experimental descriptors of activity, TOF and Ea_{app}, as well as the different selectivities. The reason for considering them as belonging to a different set, i.e., the violet point set in Scheme 3, compared to the one just discussed, which

https://doi.org/10.1021/acs.iecr.3c02512
Ind. Eng. Chem. Res. 2023, 62, 20608−20621

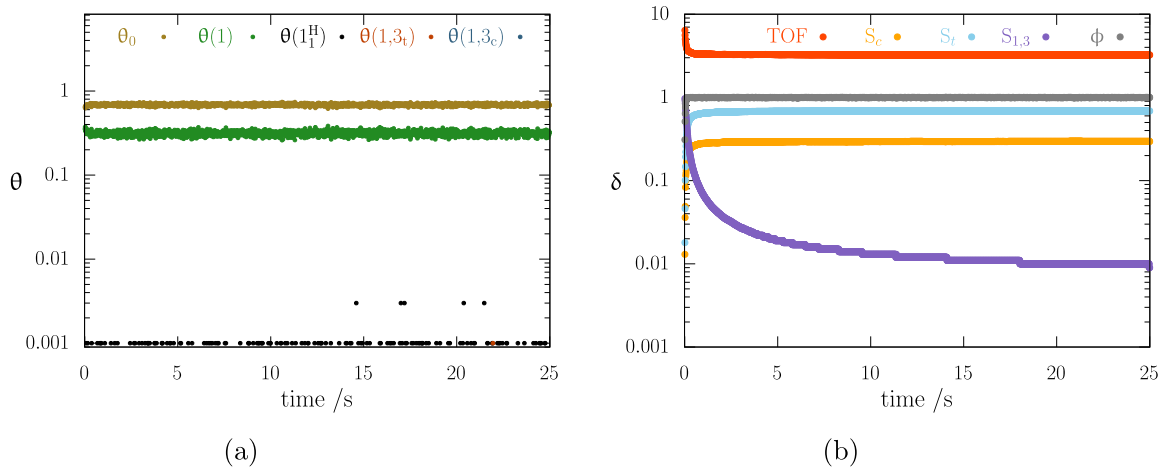

Figure 5. Descriptors θ and δ for the 0303@373 model: inset symbols show the simulated descriptors. Models 0303, similarly to the 0103 and 0503 ones, are characterized, irrespective of the temperature values, by $SS_{c/t} < 1$.

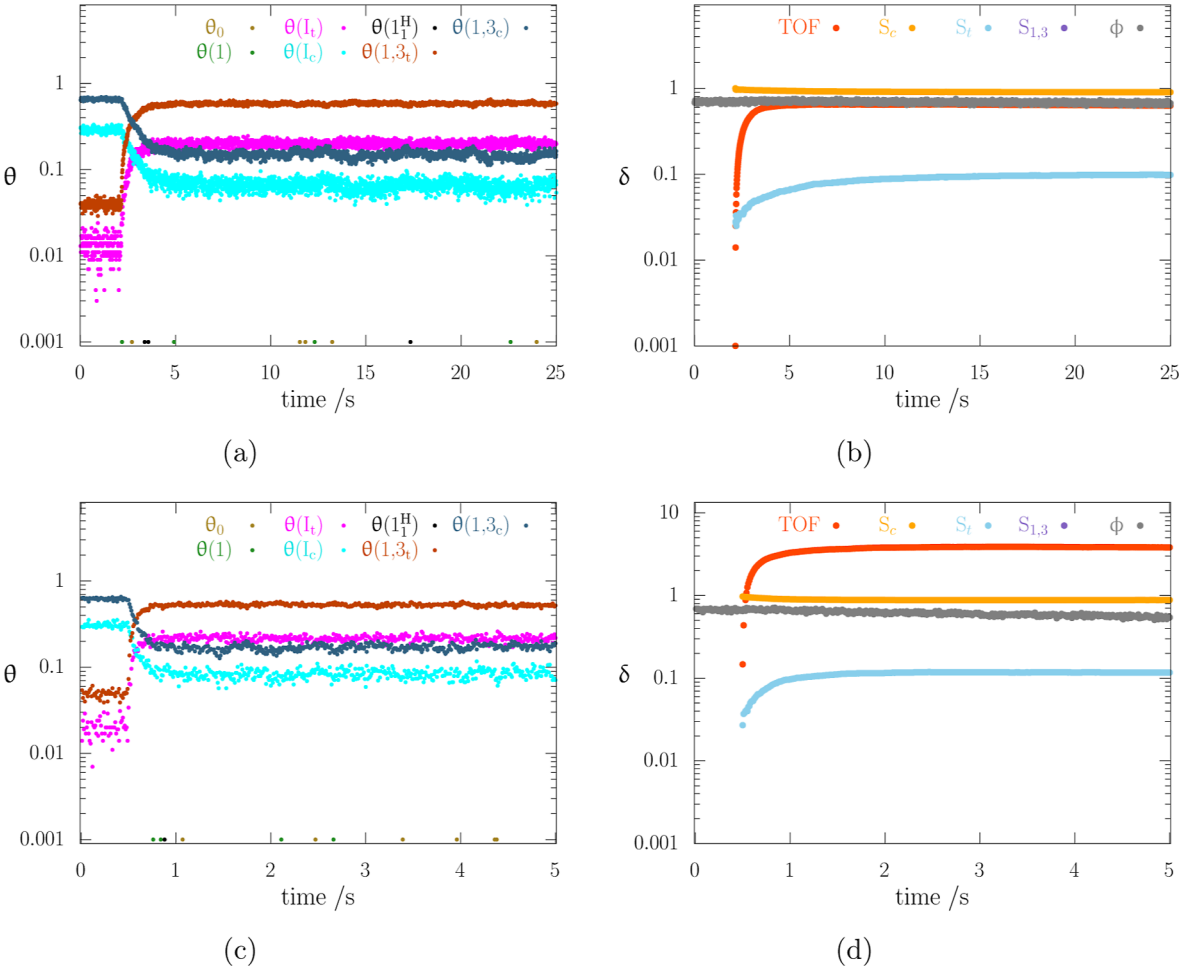

Figure 6. Descriptors θ and δ for the 0107@373—(a,b) at the top—and 0107@433—(c,d) at the bottom—models: inset symbols show the simulated descriptors whose behaviors are represented. Both of these models are characterized by $SS_{c/t} > 1$. Model 0107@433 uses the temperature experimental conditions employed in ref 45.

is individuated by the cyan points, is related to the surface population that characterizes them. As evident from Figure 5a, which illustrates the properties of the 0303@373 model, taken as an example, these systems would not have 1,3-butadiene present on the surface, and a significant portion of the surface units would be vacant, with θ_0 equal to 0.28, 0.68, and 0.92 in the order for the 0503, 0303, and 0103 models, respectively.

Given our definition of sticking probability, which leads to the "inevitable" occupation of empty surface units upon the impact of one olefin molecule, producing unactivated adsorption, and considering the extremely high value of the desorption energy of

https://doi.org/10.1021/acs.iecr.3c02512
Ind. Eng. Chem. Res. 2023, 62, 20608−20621

1,3-butadiene from the palladium {111} planes, this surface population is to be considered at least unlikely and hence determined by a combination of random factors that do not lead to a physically sound result. Indeed, the resulting mechanism remains unchanged compared with that discussed earlier. Its anomaly, however, lies in the excessive desorption of butadiene. These models are also characterized by high sticking probabilities, ranging between 0.2 and 0.9, which are not usually found due to the high degree of site occupancy generally produced by the other models studied here. On one hand, the large values of the sticking probability highlight the quite large values of θ_0, and on the other hand, it can be explained by the necessity of but-1-ene entering the surface in order for the reaction to occur.

By disregarding the origin of the surface characteristics, it can be observed that the validation of the preceding inference that the catalytic reactivity of a palladium surface in the isomerization of but-1-ene in the absence of H_2 implies the presence of the olefin and of a small amount of its monohydrogenated derivative $1_1^H(\bullet)$ on the surface, being the latter predominantly composed by hyper-hydrogenated surface units, with a notable feature in the present cases, namely the 0103, 0303, and 0503 models, where always $\phi \approx 1$ is valid.

Figure 6 illustrates the surface properties in relation to the corresponding macroscopic properties of activity and selectivity for the systems 0107@373, boxes 6a and 6b, and 0107@433, boxes 6c and 6d. The values of Ea_{app} and TOF, as shown in Table S2, are similar to those found experimentally. In this case, however, since $SS_{c/t} > 1$, the 0107 models align better with the systems studied under hydrogen deficiency by Carrà and Ragaini.[45]

Preliminarily, it should be emphasized how remarkable the ability of the proposed tdMC approach is to reproduce the variation in cis/trans stereospecificity without, as experimentally observed, substantially altering the activity values; see Tables S2 and 1.

By analyzing boxes 6a and 6c, it can be noted that the surfaces produced by the 0107 models become enriched with the surface species $I_t(*)$ and $I_c(*)$, while butene and its monohydrogenated derivative $1_1^H(\bullet)$ almost disappear. Concurrently, as shown in boxes 6b and 6d, in conjunction with the inversion of the stereoselectivity values, $SS_{c/t} > 1$, the surface butadiene disappears, while there is also a significant decrease in the fraction of the hyper-hydrogenated surface units, reduced to 0.67 and 0.54, respectively, at 373.15 and 433.15 K. These observations are clear evidence of a change in the overall picture of the reaction mechanism, caused by a reduced amount of hydrogen in the reaction system,[45] or, more precisely, of a rebalancing of the two scenarios involved in the process,[40,41] with the first scenario, the AB mechanism, becoming more relevant. This evidence substantiates and develops, for the first time, by atomistic demonstration, hypotheses on the but-1-ene isomerization already outlined by Rooney and Webb[40] in 1964.

A clear correlation appears between the surface population and the significance of the two scenarios in the whole isomerization mechanism of but-1-ene. The latter should indeed be understood as arising from the combination of these scenarios, which should not be regarded as mutually exclusive but rather as complementary. In particular, the second scenario, in the isomerization without molecular hydrogen, must necessarily arise from the first. These observations are clearly consistent with the interpretations based on experimentally supported evidence in the literature. In this regard, it is particularly important to note how the combination of $\phi \ll 1$ and $SS_{c/t} > 1$ with the prevalence of scenario 1, and $\phi \approx 1$ and $SS_{c/t} < 1$ with the prevalence of scenario 2, as well as the origin of surface hydrogen from the formation of butadiene derivatives, are remarkable computational findings that atomistically explain crucial experimental hypotheses.[40,41,45] To conclude, we could summarize—with Ragaini,[41] who proposed this hypothesis for platinum catalysts and metals belonging to its group under high temperatures and long contact times—inferring the existence of a self-hydrogenation equilibrium, a kind of dismutation representable as 2 butene ⇌ butane + butadiene, going along with the isomerization of but-1-ene and the possible presence of surface byproducts and eventually carbonaceous deposits.

For the sake of completeness, the behavior of the systems can be evaluated when both parameters, h_p and S_p, take values of either 0.0 or 1.0, respectively, corresponding to 0000 and 1010 models. The simulation results at 373.15 K for the first model and 513.15 K for the second model are shown in Figure S1. The temperature of the 1010@513 model replicates the experimental conditions, which were chosen to bypass the low reactivity inherent in butene isomerization in the absence of molecular hydrogen.[45]

The simulation of the 0000@373 model, corresponding to a simulated system in which every surface event has the same probability of occuring, exhibits unrealistically high reactivity and a widely scattered distribution of the surface molar ratios of the different surface species, resulting in significant background noise. On the other hand, the simulation of the 1010@513 model, corresponding to a simulated system whose surface events are not corrected for both steric and entropic effects, demonstrates a smaller set of surface species characterized by θ points with low dispersion and the absence of catalytic activity, TOF = 0, despite the fraction of hyper-hydrogenated surface units being close to one, $\phi \approx 1$.

The examination of these two final models reaffirms, in order to mimic experimental conditions, the importance of the two parameters, h_p and S_p, which, in the simplified perspective presented here, reproduce the steric and entropic effects related to the surface species. It also highlights how when these parameters are not taken into account, the mechanism should reduce to the occurrence of only a portion of it, specifically the first scenario, leading to the inhibition of the process with the sole production of butadiene on the surface.

CONCLUSIONS AND FUTURE DIRECTIONS

The isomerization of but-1-ene in the absence of molecular hydrogen on palladium has been studied by a new time-dependent Monte Carlo, tdMC, approach. The tdMC simulations were based on surface event probabilities derived by the activation barrier calculated in the DFT framework from vibrational zero-point corrected energy, ZPE, values concerning reactants, intermediates, transition states, and products. The uncalculated, fitting parameters employed were two: h_p and S_p. In order, these parameters mimick effects connected to (i) lateral/steric interactions and (ii) entropic effects in the processes involving desorption phenomena of surface species. Simulations captured, for the most part, all the main features of the deceptively simple but-1-ene isomerization processes, giving an atomistic explanation of the intrinsic complexity of the reaction mechanisms involved. The tdMC modeling, in particular, confirmed the experimental intuition that the whole reaction is composed of two head pathways, in the literature called abstraction, AB, and addition, AD, mechanisms, and here

https://doi.org/10.1021/acs.iecr.3c02512
Ind. Eng. Chem. Res. 2023, 62, 20608−20621

the first and second scenarios further demonstrating that these pathways play a complementary role in determining the overall mechanism and that their importance is ruled by the relative presence of hydrogen, generated by the dehydrogenation of butene to butadiene on the surface through the first scenario. The quantum-chemical characterization, in addition to providing structural and energetic information about surface species, has also opened up new perspectives in determining the nature of the species adsorbed on the surface and specifically their role in interpreting the structure-sensitive mechanism previously proposed in the literature. These findings implicitly highlight the significance of the parameters used related to the steric hindrance of the surface species and the entropic effects, both affecting the equilibrium of the reagents. The two fitting parameters above were actually adjusted on the basis of chemical intuition following an experimental design. In the future, in addition to replicating various experimental conditions and further comparing the hypothesized properties of the surface species based on experimental evidence with those determined via quantum chemistry, it would be desirable to integrate a subroutine within the tdMC framework focused on efficiently optimizing the values of h_p and S_p. However, the authors believe that this special revision in the code would not lead to substantial changes in the structure of the current work and its conclusions. The subroutine could also be tasked with determining different descriptors, such as the apparent order of reaction of the different actors present in the catalytic processes and reproducing the effects of surface carbonaceous deposits formed during the reaction due to the aging of the catalyst. Maintaining the tasks expressed in the rows just above, it is also possible to think, in a more ambitious context, of suppressing these parameters: h_p, in this case, could be obtained by DFT calculations actually oriented to the evaluation of the influence of the lateral interactions characterizing the different surface species involved, while S_p could not perhaps be necessary if the here ZPE- were replaced by a ΔG-based approach.

■ ASSOCIATED CONTENT

Supporting Information

The Supporting Information is available free of charge at https://pubs.acs.org/doi/10.1021/acs.iecr.3c02512.

tdMC code flow chart highlighting the role of *RNGs*; relative occurrence probabilities; literature and simulated TOF and apparent activation energies; and descriptors θ and δ for the 0000@373 and 1010@513 models (PDF)

■ AUTHOR INFORMATION

Corresponding Author

Dario Duca − *Dipartimento di Fisica e Chimica "Emilio Segrè"—Università degli Studi di Palermo, Palermo I-90128, Italy*; orcid.org/0000-0003-0281-8634; Email: dario.duca@unipa.it

Authors

Francesco Ferrante − *Dipartimento di Fisica e Chimica "Emilio Segrè"—Università degli Studi di Palermo, Palermo I-90128, Italy*; orcid.org/0000-0002-2989-4365

Marco Bertini − *Dipartimento di Fisica e Chimica "Emilio Segrè"—Università degli Studi di Palermo, Palermo I-90128, Italy*

Laura Gueci − *Dipartimento di Fisica e Chimica "Emilio Segrè"—Università degli Studi di Palermo, Palermo I-90128, Italy*; orcid.org/0000-0002-7837-2037

Complete contact information is available at: https://pubs.acs.org/10.1021/acs.iecr.3c02512

Notes

The authors declare no competing financial interest.

■ ACKNOWLEDGMENTS

D.D. thanks Tamás Vidoczy and Dmitry Murzin for their long friendship and for the inspiration given, along the way, to the development of the topics of this work, which is dedicated to them and to the memory of Vladimir Elokhin, also his friend and pioneer in the catalysis Monte Carlo field.

■ ADDITIONAL NOTES

[1]In this study, the time unit will be referred to as the hitting frequency of but-1-ene. In fact, given the model assumption that a surface event can only occur if it is activated by the "blast" following the hit of one reactant molecule, no other reaction event can be more frequent than the same but-1-ene hitting. This, therefore, fixes the smallest time unit related to the reaction events and ensures that no meaningful events are overlooked. A more frequent event could be the hitting of a possible eluant gas, such as Ar in the title simulations. This occurrence, pertaining to an inert species, can be related to a null event, whose use as a reference for the time unit would impose a computational burden without yielding substantial insights.

[2]To avoid misunderstandings between the terms isomer and pseudo-isomer, either gas or surface isomers will not be collectively set while they will be specifically named using their prefixes, e.g., cis and trans.

[3]Given the definition of the i-th species, it is evident that the index i in the summation of eqs 3 and 4 does not include the source species l. The probability of the backward reaction from k to l in these equations is instead connected to the term: $\exp\left(-\frac{\varepsilon_{kl}-\varepsilon_{kl}}{k_B T}\right)=1$.

■ REFERENCES

(1) Cortés, J.; Valencia, E.; Araya, P. Monte Carlo simulations and kinetic theory of homogeneous and heterogeneous adsorption with lateral interactions. *J. Chem. Phys.* **1994**, *100*, 7672−7676.

(2) Dawnkaski, E. J.; Srivastava, D.; Garrison, B. J. Time dependent Monte Carlo simulations of H reactions on the diamond {001}(2×1) surface under chemical vapor deposition conditions. *J. Chem. Phys.* **1995**, *102*, 9401−9411.

(3) Dawnkaski, E.; Srivastava, D.; Garrison, B. Time-dependent Monte Carlo simulations of radical densities and distributions on the diamond {001} (2 × 1): H surface. *Chem. Phys. Lett.* **1995**, *232*, 524−530.

(4) (a) Duca, D.; Botár, L.; Vidóczy, T. Monte Carlo simulation of ethylene hydrogenation on Pt catalysts. *J. Catal.* **1996**, *162*, 260−267. (b) Duca, D.; Baranyai, P.; Vidóczy, T. Monte-Carlo model for the hydrogenation of alkenes on metal catalyst. *J. Comput. Chem.* **1998**, *19*, 396−403.

(5) Duca, D.; La Manna, G.; Russo, M. R. Computational studies on surface reaction mechanisms: ethylene hydrogenation on platinum catalysts. *Phys. Chem. Chem. Phys.* **1999**, *1*, 1375−1382.

(6) (a) Pal, S.; Landau, D. P. Monte Carlo simulation and dynamic scaling of surfaces in MBE growth. *Phys. Rev. B* **1994**, *49*, 10597−10606. (b) Asada, T.; Nishimoto, K. Monte Carlo simulations of $M^+Cl^-(H_2O)_n$ (M = Li, Na) clusters and the dissolving mechanism of

ion pairs in water. *Chem. Phys. Lett.* **1995**, *232*, 518−523. (c) Garrison, B. J.; Kodali, P. B. S.; Srivastava, D. Modeling of surface processes as exemplified by hydrocarbon reactions. *Chem. Rev.* **1996**, *96*, 1327−1342.

(7) (a) Barone, G.; Duca, D. Hydrogenation of 2,4-dinitro-toluene on Pd/C catalysts: computational study on the influence of the molecular adsorption modes and of steric hindrance and metal dispersion on the reaction mechanism. *J. Catal.* **2002**, *211*, 296−307. (b) Barone, G.; Duca, D. Ab initio study of structure and energetics of species involved in the 2,4-dinitro-toluene hydrogenation on Pd catalysts. *J. Mol. Struct.: THEOCHEM* **2002**, *584*, 211−220. (c) Barone, G.; Duca, D. New time-dependent Monte Carlo algorithm designed to model three-phase batch reactor processes: applications on 2,4-dinitro-toluene hydrogenation on Pd/C catalysts. *Chem. Eng. J.* **2003**, *91*, 133−142. (d) Barone, G.; Duca, D. Erratum to "New time-dependent Monte Carlo algorithm designed to model three-phase batch reactor processes: applications on 2,4-dinitro-toluene hydrogenation on Pd/C catalysts" [Chem. Eng. J. 91 (2003) 133−142]. *Chem. Eng. J.* **2003**, *95*, 251.

(8) (a) Duca, D.; Varga, Zs.; La Manna, G.; Vidóczy, T. Hydrogenation of acetylene-ethylene mixtures on Pd catalysts: study of the surface mechanism by computational approaches. Metal dispersion and catalytic activity. *Theor. Chem. Acc.* **2000**, *104*, 302−311. (b) Duca, D.; Barone, G.; Varga, Zs. Hydrogenation of acetylene-ethylene mixtures on Pd catalysts: computational study on the surface mechanism and on the influence of the carbonaceous deposits. *Catal. Lett.* **2001**, *72*, 17−23.

(9) Duca, D.; Barone, G.; Giuffrida, S.; Varga, Zs. IDEA: Interface dynamics and energetics algorithm. *J. Comput. Chem.* **2007**, *28*, 2483−2499.

(10) Giuffrida, S.; Barone, G.; Duca, D. Adsorbed CO on Group 10 Metal Fragments: A DFT Study. *J. Chem. Inf. Model.* **2009**, *49*, 1223−1233.

(11) Boudart, M. Adsorption assisted desorption in catalytic cycles. *J. Mol. Catal. A: Chem.* **1999**, *141*, 1−7.

(12) Wintterlin, J.; Schuster, R.; Ertl, G. Existence of a "hot" atom mechanism for the dissociation of O_2 on Pt(111). *Phys. Rev. Lett.* **1996**, *77*, 123−126.

(13) (a) Fichthorn, K. A.; Weinberg, W. H. Theoretical foundations of dynamical Monte Carlo simulations. *J. Chem. Phys.* **1991**, *95*, 1090−1096. (b) Šomvársky, J.; Dušek, K. Kinetic Monte-Carlo simulation of network formation. *Polym. Bull.* **1994**, *33*, 369−376.

(14) Chatterjee, A.; Vlachos, D. G. An overview of spatial microscopic and accelerated kinetic Monte Carlo methods. *J. Comput.-Aided Mater. Des.* **2007**, *14*, 253−308.

(15) Stamatakis, M.; Vlachos, D. G. Unraveling the complexity of catalytic reactions via kinetic Monte Carlo simulation: current status and frontiers. *ACS Catal.* **2012**, *2*, 2648−2663.

(16) (a) Patel, P.; Wells, R. H.; Kaphan, D. M.; Delferro, M.; Skodje, R. T.; Liu, C. Computational investigation of the role of active site heterogeneity for a supported organovanadium(III) hydrogenation catalyst. *ACS Catal.* **2021**, *11*, 7257−7269. (b) Li, X.; Grabow, L. C. Evaluating the benefits of kinetic Monte Carlo and microkinetic modeling for catalyst design studies in the presence of lateral interactions. *Catal. Today* **2022**, *387*, 150−158.

(17) (a) Fajín, J. L. C.; Moura, A. S.; Cordeiro, M. N. D. S. First-principles-based kinetic Monte Carlo simulations of CO oxidation on catalytic Au(110) and Ag(110) surfaces. *Phys. Chem. Chem. Phys.* **2021**, *23*, 14037−14050. (b) Díaz López, E.; Comas-Vives, A. Kinetic Monte Carlo simulations of the dry reforming of methane catalyzed by the Ru (0001) surface based on density functional theory calculations. *Catal. Sci. Technol.* **2022**, *12*, 4350−4364.

(18) Rothemberg, G. *Catalysis*; John Wiley & Sons, Ltd, 2008; Chapter 2, pp 39−75.

(19) Delbecq, F.; Zaera, F. Origin of the selectivity for trans-to-cis isomerization in 2-butene on Pt(111) single crystal surfaces. *J. Am. Chem. Soc.* **2008**, *130*, 14924−14925. PMID: 18937459

(20) (a) Barone, G.; Armata, N.; Prestianni, A.; Rubino, T.; Duca, D.; Murzin, D. Yu. Confined but-2-ene catalytic isomerization inside H-ZSM-5 models: a DFT study. *J. Chem. Theory Comput.* **2009**, *5*, 1274−1283. (b) Ferrante, F.; Rubino, T.; Duca, D. Butene isomerization and double-bond migration on the H-ZSM-5 outer surface: a density functional theory study. *J. Phys. Chem. C* **2011**, *115*, 14862−14868.

(21) Li, Y.; Ma, C.; Yang, H.; Zhang, Z.; Zhang, X.; Qiao, N.; Wang, J.; Hao, Z. Room-temperature isomerization of 1-butene to 2-butene over palladium-loaded silica nanospheres catalyst. *Chem. Eng. J.* **2016**, *299*, 1−7.

(22) Choudhary, V. R.; Doraiswamy, L. Isomerization of n-butene to isobutene: I. Selection of catalyst by group screening. *J. Catal.* **1971**, *23*, 54−60.

(23) (a) Brandt, B.; Fischer, J.-H.; Ludwig, W.; Libuda, J.; Zaera, F.; Schauermann, S.; Freund, H.-J. Isomerization and hydrogenation of cis-2-butene on Pd model catalyst. *J. Phys. Chem. C* **2008**, *112*, 11408−11420. (b) D'Anna, V.; Duca, D.; Ferrante, F.; La Manna, G. DFT studies on catalytic properties of isolated and carbon nanotube supported Pd_9 cluster Part II. Hydro-isomerization of butene isomers. *Phys. Chem. Chem. Phys.* **2010**, *12*, 1323−1330. (c) Markova, V. K.; Philbin, J. P.; Zhao, W.; Genest, A.; Silvestre-Albero, J.; Rupprechter, G.; Rösch, N. Catalytic transformations of 1-butene over palladium. A combined experimental and theoretical study. *ACS Catal.* **2018**, *8*, 5675−5685. (d) Genest, A.; Silvestre-Albero, J.; Li, W.-Q.; Rösch, N.; Rupprechter, G. The origin of the particle-size-dependent selectivity in 1-butene isomerization and hydrogenation on Pd/Al_2O_3 catalysts. *Nat. Commun.* **2021**, *12*, 6098.

(24) Soler, J. M.; Artacho, E.; Gale, J. D.; Garcia, A.; Junquera, J.; Ordejón, P.; Sánchez-Portal, D. The SIESTA method for ab initio order-N materials simulation. *J. Phys.: Condens. Matter* **2002**, *14*, 2745−2779.

(25) van Setten, M. J.; Giantomassi, M.; Bousquet, E.; Verstraete, M. J.; Hamann, D. R.; Gonze, X.; Rignanese, G.-M. The PseudoDojo: Training and grading a 85 element optimized norm-conserving pseudopotential table. *Comput. Phys. Commun.* **2018**, *226*, 39−54.

(26) Garcia, A.; Verstraete, M. J.; Pouillon, Y.; Junquera, J. The PSML format and library for norm-conserving pseudopotential data curation and interoperability. *Comput. Phys. Commun.* **2018**, *227*, 51−71.

(27) Ferrante, F.; Prestianni, A.; Bertini, M.; Duca, D. H_2 transformations on graphene supported palladium cluster: DFT-MD simulations and NEB calculations. *Catalysts* **2020**, *10*, 1306.

(28) Bertini, M.; Ferrante, F.; Duca, D. Empathes: a general code for nudged elastic band transition states search. *Comput. Phys. Commun.* **2022**, *271*, 108224.

(29) Henkelman, G.; Jónsson, H. Improved tangent estimate in the nudged elastic band method for finding minimum energy paths and saddle points. *J. Chem. Phys.* **2000**, *113*, 9978−9985.

(30) Henkelman, G.; Uberuaga, B. P.; Jónsson, H. A climbing image Nudged Elastic Band Method for finding saddle points and minimum energy paths. *J. Chem. Phys.* **2000**, *113*, 9901−9904.

(31) Ziff, R. M.; Gulari, E.; Barshad, Y. Kinetic phase transitions in an irreversible surface-reaction model. *Phys. Rev. Lett.* **1986**, *56*, 2553−2556.

(32) In the development of the current Monte Carlo model, instead of collisions determining local "blasts" leading to surface transformations, one could contemplate just the random selection of a generic reaction site. At this site, various transformations, each with its own probability of occurrence, may take place after a specific unit of time has elapsed, monitored by the impact of specific molecules on the surface. Although the simulation results would remain consistent, this approach would neglect the local release of energy. Conversely, it is reasonable to assume that the molecule adsorbed at the impacted region of the surface is the "activated" one, and thus more inclined to undergo transformation compared to others.

(33) It is preferable to refer to the expression "catalytically active surface unit" or, more simply, to the shortened form "surface unit" and not to the expression surface-site since, as shown in the body of the discussion, the surface species interact with clusters or group of sites rather than individually with single sites.

(34) The sticking probability of a molecular species has been also defined as the fraction of adsorbed and not-desorbed molecules

https://doi.org/10.1021/acs.iecr.3c02512
Ind. Eng. Chem. Res. 2023, 62, 20608−20621

compared to the total number of molecular collisions within the time interval between two consecutive measurements, see ref 48.
(35) Dugundji, J.; Ugi, I. *Computers in Chemistry*; Springer: Berlin, Heidelberg, 1973, pp 19−64.An algebraic model of constitutional chemistry as a basis for chemical computer programs
(36) In early Monte Carlo models reported in catalytic literature, the catalyst surface was often simulated using a matrix in which its elements represented occupied or unoccupied sites (or group of sites) of the catalyst. These matrix elements were stochastically sampled to determine, based on the occupancy nature and topology information related to them, which transformation should occur and on which sites.
(37) Flannery, B. P.; Press, W. H.; Vetterling, W. T.; Teukolsky, S. A. *Numerical Recipes in Fortran 90*; Cambridge University Press: Cambridge, 2002; Chapter B7, pp 1141−1143.
(38) Kozuch, S.; Shaik, S. A Combined kinetic-quantum mechanical model for assessment of catalytic cycles: application to cross-coupling and Heck reactions. *J. Am. Chem. Soc.* **2006**, *128*, 3355−3365.
(39) Dumesic, J.; Rudd, D.; Aparicio, L.; Rekoske, J.; Trevino, A. *ACS Professional Reference Book*; Wiley, 1993, pp 36−37.The Microkinetics of Heterogeneous Catalysis
(40) Rooney, J. J.; Webb, G. The importance of π-bonded intermediates in hydrocarbon reactions on transition metal catalysts. *J. Catal.* **1964**, *3*, 488−501.
(41) Ragaini, V. The isomerization of n-butenes over platinum black in the absence of molecular hydrogen. *J. Catal.* **1974**, *34*, 1−6.
(42) Gueci, L.; Ferrante, F.; Prestianni, A.; Arena, F.; Duca, D. Structural, energetic and kinetic database of catalytic reactions: Benzyl alcohol to benzaldehyde oxidation on MnO_x clusters. *Data Brief* **2021**, *38*, 107369.
(43) Wells, P.; Wilson, G. Butene isomerization catalyzed by supported metals in the absence of molecular hydrogen. *J. Catal.* **1967**, *9*, 70−75.
(44) Holbrook, L.; Wise, H. Role of hydrogen in butene isomerization catalyzed by supported and unsupported palladium. *J. Catal.* **1972**, *24*, 315−319.
(45) Carrà, S.; Ragaini, V. On the mechanism of 1-butene isomerization on supported palladium. *J. Catal.* **1968**, *10*, 230−237.
(46) Duca, D.; Liotta, L.; Deganello, G. Selective Hydrogenation of Phenylacetylene on Pumice-Supported Palladium Catalysts. *J. Catal.* **1995**, *154*, 69−79.
(47) Markova, V. K.; Philbin, J. P.; Zhao, W.; Genest, A.; Silvestre-Albero, J.; Rupprechter, G.; Rösch, N. Catalytic Transformations of 1-Butene over Palladium. A Combined Experimental and Theoretical Study. *ACS Catal.* **2018**, *8*, 5675−5685.
(48) Lytken, O.; Lew, W.; Harris, J. J. W.; Vestergaard, E. K.; Gottfried, J. M.; Campbell, C. T. Energetics of Cyclohexene Adsorption and Reaction on Pt(111) by Low-Temperature Microcalorimetry. *J. Am. Chem. Soc.* **2008**, *130*, 10247−10257.

https://doi.org/10.1021/acs.iecr.3c02512
Ind. Eng. Chem. Res. 2023, 62, 20608−20621